

## Analysis of boron in biological reference materials using prompt gamma activation analysis

Hyun-Je Cho, Yong-Sam Chung, Young-Jin Kim

*Korea Atomic Energy Research Institute, KAERI, Daejeon, Korea*

(Received July 26, 2004)

A prompt gamma activation analysis facility has been constructed on the ST1 horizontal beam port at the HANARO research reactor, KAERI in 2003. The detector system consists of a high-purity Ge detector surrounded by BGO/NaI(Tl) scintillators as an annulus type to reject the Compton scattered photons. Detection sensitivity for boron was obtained from the prompt gamma-ray spectra of boric acid, B(OH)<sub>3</sub>, containing 0.1–65 µg boron. The net peak for the calculation of the boron concentration was obtained by eliminating the sodium 472 keV peak, involved in the boron 478 keV peak. The biological samples used are NIST SRMs such as Peach Leaves, Apple Leaves, Tomato Leaves, Spinach Leaves, Total Diet, Typical Diet, Oyster Tissue and Corn Bran, etc. The measured values for high boron concentration showed up to a 3% of the relative, but in a low concentration below 5 ppm, present values were higher than the certified ones.

### Introduction

Boron is known as an essential trace element for the growth of plants. It is in charge of the uracil formation and normal growth and its deficiency as well as toxicity threatens crop productivity in many areas.<sup>1</sup> It has been reported that boron affects the metabolism of calcium, phosphorus and magnesium in animals.<sup>2</sup> Boron is present in animal tissue in low concentrations (about 1 ppm) and is probably an essential micronutrient for humans. Though the essentiality of boron for animals is not yet fully established,<sup>3</sup> there is growing evidence that it may have a metabolic role in human and animal nutrition.<sup>4,5</sup> Its deficiency in plants may result in a reduced growth, yield loss, and even death, depending on the severity of the deficiency. In contradiction to this, an excess of boron in food products and drinking water is toxic to plants and animals, which is also considered harmful for health.<sup>6</sup>

Early on, there were many investigations on the micro-analysis of boron in various materials. Boron occurs as an impurity in steels, a major component in glass, a thermalizing agent in nuclear reactor materials such as boron carbide of control rods, a detecting system for neutrons, a nutrient element in biological and environmental samples and a dopant in silicon wafers and semiconductor devices.<sup>7</sup> Boron is also used as a source for the short range alpha-particles in cancer treatment using boron neutron capture therapy (BNCT).<sup>8,9</sup> In the determination of boron using a PGAA system, the accuracy, precision and detection limits have been evaluated.<sup>10</sup> In prompt gamma activation analysis (PGAA), boron concentrations in tumors, tissues, blood and cultured cells were estimated from the calibration curves obtained by using standard samples

containing different <sup>10</sup>B concentrations by MATSUMOTO et al.<sup>11</sup> Recently, the determination of boron in marine carbonates and coral samples by PGAA was reported.<sup>12</sup> ANDERSON et al.<sup>13</sup> has measured the intake of the boron in foods. They showed that the higher boron concentrations in drinking water, fruit and, vegetable consumption increase the boron intake.

Boron has a low atomic number, and because its nuclear properties, it is difficult to determine by neutron activation analysis, atomic absorption spectrometry, particle induced X-ray emission spectrometry or by X-ray fluorescence spectrometry, and also chemical methods are not suitable for the determination of boron at low levels. Because low boron concentrations are relatively difficult to determine using other chemical methods, a method with a high precision and low detection limit is required to determine the content and the isotope composition of boron in biological materials. Therefore, prompt gamma neutron activation analysis (PGAA), which as a non-destructive method requires no special sample preparation, is suggested as an appropriate analytical method. The aim of the present study is to confirm the accuracy of the boron analysis in biological samples using the PGAA system at the HANARO research reactor, KAERI.

### Experimental

#### *PGAA facility*

The prompt gamma neutron activation analysis system at the HANARO research reactor, KAERI in Korea, has been modified in 2003 to obtain a high quality neutron flux and a low background. A diffracted thermal neutron beam is extracted by using pyrolytic graphite (PG) crystals by Bragg diffraction with the

Bragg angle set at  $45^\circ$ . To reduce the influence of background by scattered neutrons, enriched lithium tiles ( $^6\text{LiF}$ ) were attached to the front of the HPGe detector in the direction of the gamma-ray emitted from the sample. The neutron flux and Cd-ratio for gold at the sample position are  $8.4 \cdot 10^7 \text{ n} \cdot \text{cm}^{-2} \cdot \text{s}^{-1}$  and above 300, respectively. Flux uniformity was within 4% for the central area of  $1 \times 1 \text{ cm}^2$  of the total beam cross section of  $2 \times 2 \text{ cm}^2$ .<sup>14</sup>

In the measurement of emitted prompt gamma-rays, the detection system was composed of a HPGe detector (GEM-30190 EG&G Ortec, relative efficiency 43%) surrounded by eight bismuth-germanate ( $\text{Bi}_4\text{Ge}_3\text{O}_{12}$ : BGO) detectors plus two NaI(Tl) scintillators (5.75HW6.30 BGO/NaI(Tl)/(8) 1.5-x, BICRON) in order to reject the Compton-scattered photons.<sup>14</sup> The LiF tiles as a shielding material in the sample chamber were used to avoid scattered neutrons towards the detector and 10 cm thick lead bricks were used for the reduction of the gamma-ray background. For the maintenance of a low background condition, the sample is sealed into a Teflon vial and suspended with a string on the Teflon frame of the folder. The gamma-ray detector is located at about 25 cm from the sample and at  $90^\circ$  to the beam direction. The BGO/NaI(Tl) detectors are covered with an aluminum case and are shielded by 10 cm of lead to stop gamma-ray appearing from the surrounding near the scintillation detector. The main specifications are referred to in previous works.<sup>14</sup>

#### *Sample preparation*

The powdered samples were dried using an oven at  $30^\circ\text{C}$  for 2 hours and then cooling to room temperature. The sample was put into a polytetrafluoroethylene (PTFE) vial with lid and stored in a desiccator. To check the moisture content, the sample was weighed before and after drying. The moisture content of sample was less than 1.5%. Each of the biological samples used was measured five times with two or three sample weights, respectively. The biological samples used are the followings: Peach Leaves (NIST SRM 1547) with a weight of 12, 30 and 85 mg, Apple Leaves (NIST SRM 1515) with a weight of 5, 12 and 27 mg, Spinach Leaves (NIST SRM 1570a) with a weight of 4, 22 and 30 mg, Tomato Leaves (NIST SRM 1573a) with a weight of 12 and 25 mg, Total Diet (NIST SRM 1548) with weight of 6 and 38 mg, Typical Diet (NIST SRM 1548a) with a weight of 25 and 40 mg, the Oyster Tissue (NIST SRM 1566b) with a weight of 5 and 11 mg, and Corn Bran (NIST SRM 8433) with a weight of 25 and 39 mg.

#### *Analysis of boron*

The PTFE vial of cylindrical shape was 8 mm in outer diameter, 1 mm in thickness and 5 mm in height.

The vial size was made to be less than the beam dimensions and then the irradiation was performed in air. The sample frame was inclined  $45^\circ$  with respect to the diffracted beam direction. All the samples were measured for 3,600 seconds per sample at the same sample position.

The full energy peak efficiency of the detector was calibrated by the conventional method using standard radioactive sources. A 43% HPGe detector connected to a PC based 16k MCA is used for counting the prompt gamma-rays. The resolution of the detector has been 2.3 keV at 1332 keV of  $^{60}\text{Co}$ . The MCA has been calibrated in the region up to 10 MeV using the gamma-rays from  $^{152}\text{Eu}$ ,  $^{60}\text{Co}$  and  $^{36}\text{Cl}$ . The data on the absolute gamma-ray intensities for the above isotopes were taken from IAEA-TECDOC-619.<sup>15</sup> The absolute full energy peak efficiencies were determined for the low energy region using a  $^{152}\text{Eu}$  source and the relative efficiency plot for the energy region from 0.5 to about 10 MeV obtained from the prompt gamma-ray spectrum of  $^{35}\text{Cl}(n,\gamma)$  and  $^{14}\text{N}(n,\gamma)$ . The typical efficiency values are in the order of  $10^{-4}$  to  $10^{-5}$ .<sup>14</sup> Full energy peak efficiency is determined by polynomial fitting; the standard uncertainty is less than 3% in the low energy region, and less than 5% for the overall spectrum. Non-linearity of the spectrometer is determined in a similar manner by fitting a polynomial function to the observed data for accurately obtained gamma-ray lines. Dilute boric acid was used to prepare the solid samples, and a sensitivity of  $1468 \text{ counts} \cdot \text{s}^{-1} \cdot (\text{mg B})^{-1}$  was derived from the 478 keV Doppler-broadened peak.

### **Results and discussion**

The boron peak can be overlapped with the prompt gamma-rays from  $^{24}\text{Na}$  (472 keV). This contamination comes from the NaI(Tl) scintillator making up parts of the Compton-suppressed detector. The statistical fluctuation of the boron peak concealed the sodium peak in the case of a high boron content in the samples. A minor contribution results from the LiF tiles used as a neutron shielding material. In this case, the 478 keV peak from the  $^6\text{Li}(n,\gamma)^7\text{Li}$  reaction was not broadened. The most important background sources are from the sodium impurities in the detector, oxygen and nitrogen in the air, aluminum in the sample holder and fluorine from the Teflon holding the samples. Background spectra were recorded and used to correct the analysis when necessary. Major background of the present measurement occurs from the sodium in the low energy region for the boron analysis. As shown in Table 1, Compton-mode values are suppressed by a few times to single-mode values. In the boron energy region, the suppression rate,  $\Delta R(R_{\text{single}}/R_{\text{Compton}})$ , of the Compton mode is about 4–5 lower than that of a single mode. The peak of hydrogen, a 2223 keV gamma-range, is about a

5–6 lower than that of a single mode, therefore, the present measurements in the Compton mode are useful for the suppression system. The background, generally, plays an important role in the analysis of an element which has a high energy gamma-ray. For the comparison of the spectrum shape, the present measurement obtained from the Compton and single modes of the boron are used as shown in Fig. 1. In Fig. 1, a single spectrum is compared with a standard Compton-suppressed spectrum. The low energy region background due to the Compton continuum and circumference within the detector assembly is greatly reduced by improving the signal-to-background ratio, without reducing the overall precision for the strong low energy peaks. Generally, the counting rate of the boron peak area is influenced by the interference from other gamma-rays.<sup>16</sup>

Table 1. Comparison of the Compton- and the single-mode for the sodium and boron (boric acid) sample

| $\Delta E$ , MeV | Total cps |         | $\Delta R$<br>( $R_{\text{sing}}/R_{\text{Comp}}$ ) |
|------------------|-----------|---------|---|
|                  | Compton   | Single  |   |
| NaCl             |           |         |   |
| ~1               | 151.88    | 632.23  | 4.16  |
| 1–2              | 46.35     | 216.94  | 4.68  |
| 2–3              | 17.98     | 111.62  | 6.21  |
| 3–4              | 8.91      | 71.18   | 7.99  |
| 4–5              | 5.68      | 51.11   | 9.00  |
| 5–6              | 4.43      | 41.11   | 9.28  |
| 6–7              | 3.78      | 27.88   | 7.38  |
| 7–8              | 2.20      | 12.37   | 5.62  |
| Boron            |           |         |   |
| ~1               | 1542.02   | 7413.13 | 4.81  |
| 1–2              | 485.04    | 2340.95 | 4.83  |
| 2–3              | 171.10    | 1136.07 | 6.64  |
| 3–4              | 50.49     | 381.18  | 7.55  |
| 4–5              | 31.87     | 275.56  | 8.65  |
| 5–6              | 24.82     | 199.94  | 8.06  |
| 6–7              | 18.80     | 145.81  | 7.76  |
| 7–8              | 11.61     | 76.29   | 6.57  |

Table 2. Standard uncertainties estimated in boron analysis by PGAA

| Uncertainties due to                      | Uncertainty, % |
|---|----------------|
| Statistical error                         | 0.20–0.34      |
| detection efficiency                      | 2.80           |
| Mass (sample weight)                      | 0.05           |
| detection sensitivity<br>(boron solution) | 0.50           |
| Background subtraction                    |                |
| 472 keV, Na                               | 2.40–2.65      |
| 475.3 keV (unknown)                       | 1.00           |
| Total uncertainty:                        | 3.86–4.00      |

In Fig. 2, the boron peak was overlapped with the prompt gamma-rays from  $^{24}\text{Na}$  at 472 keV. This effect came from the scintillation detector making up parts of the Compton-suppressed detector. The interference is caused by the strong 472 keV gamma-ray arising from the capture in sodium. There are other capture gamma-rays (e.g., 91 keV) in sodium whose large intensity values are relative to that of the 472 keV gamma-ray. The results are either known from the literature or can be determined experimentally using the standards. These intensity ratios can be used to subtract the appropriate counts from the combined boron plus the sodium peak in the 468–487 keV region. The effect of interference from lithium [ $^6\text{Li}(n,\gamma)^7\text{Li}$ ] can also appear,<sup>17</sup> but at high boron concentration, the peak shape of lithium appeared weakly in the boron region and the count ratio was below 1.5% within the boron broaden peak area. At low boron concentration below 5 ppm, the lithium peak of 477.6 keV has an effect on the boron peak. The analysis results reconsidered about its effect showed the count ratio of lithium in the broaden peak area to be about 3–5%. The region of interest is decomposed into a broad peak, interfering normal peaks and a background. The statistical fluctuation of the boron peak can neglect the sodium peak in the case of a high boron content in the samples. Considering the small thermal neutron cross-section (38 mb) of the nuclear reaction, the influence of this peak was significant only at low boron concentrations (<5 ppm).

The combined uncertainties were in the range of 3.86 to 4.0% for boron analysis in the relevant materials. The main sources of the uncertainties are due to statistical errors (0.20–0.34%), the detection efficiency (2.8%), the background subtraction of 472 keV Na (2.4–2.65%), and error sources including some other corrections, as shown in Table 2. The boron concentration in each sample was determined from the measured count rate of the boron peak, sample mass and boron sensitivity. The results are summarized in Table 3 together with the certified values. The relative errors of the measured values are 1.0–3.0% for Apple Leaves, Tomato Leaves, Spinach Leaves and Peach Leaves, 13% for the Typical Diet, about 40% for Total Diet, Oyster Tissue, and Corn Bran. The analysis of boron using the present PGAA facility is in good agreement with the certified value of NIST SRMs above 10 ppm, but below 5 ppm concentration, the measured values are higher than the certified values. Figure 3 shows the Z-score from each value. Comparison between experimental results and certified values was done in terms of the ratio of experiment to certified values.

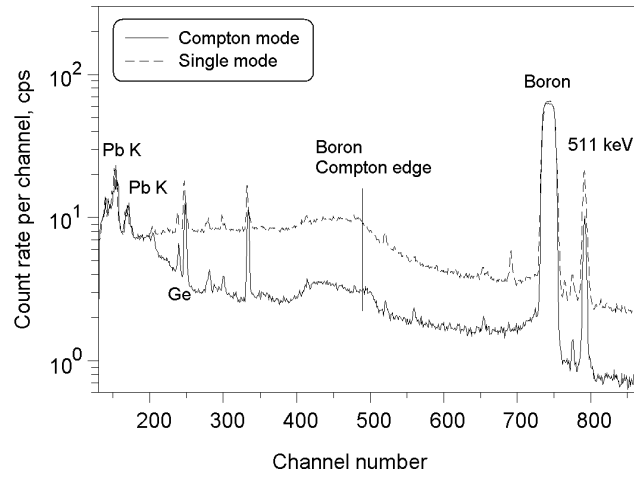


Fig. 1. Spectrum of the  $\gamma$ -rays emitted from NIST SRM (Spinach Leaves)

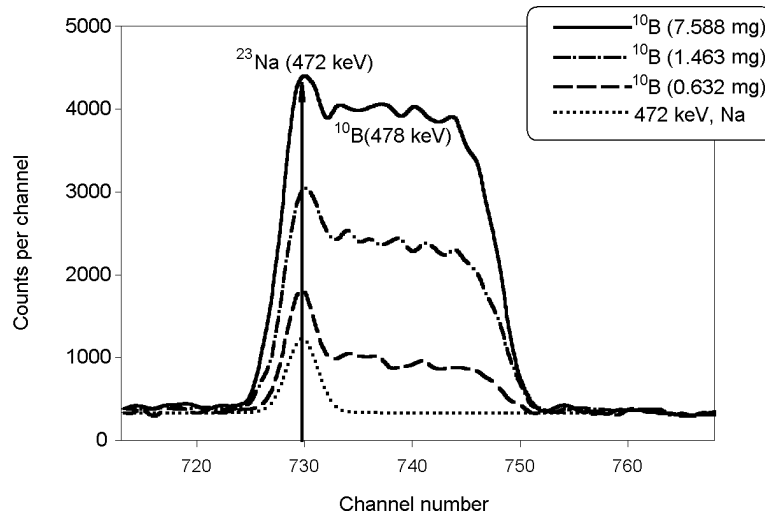


Fig. 2. Part of the prompt gamma-ray spectra near the boron peak for various boron concentrations

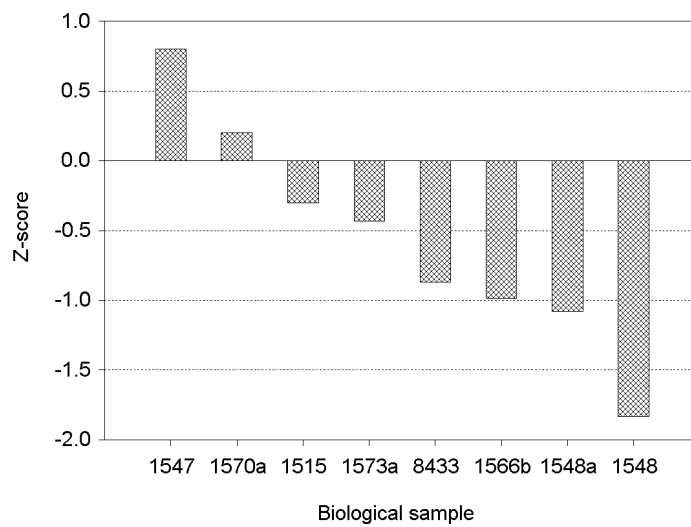


Fig. 3. Comparison of the analytical results for biological NIST SRMs

Table 3. Comparison between the measured values and certified values for NIST SRM samples

| Sample (NIST SRM)     | Present,<br>ppm | Certified,<br>ppm | Others,<br>ppm   |
|-----------------------|-----------------|-------------------|--|
| Peach (1547)          | 28.2 ± 1.00     | 29.0 ± 2.00       | 27.6 ± 2.80 <sup>18a</sup><br>26.2 ± 1.00 <sup>19e</sup> |
| Apple (1515)          | 27.3 ± 1.00     | 27.0 ± 2.00       | 28.6 ± 3.70 <sup>19e</sup>                               |
| Spinach (1570a)       | 37.3 ± 1.50     | 37.6 ± 1.00       | 30.1 ± 3.50 <sup>20b</sup>                               |
| Total Diet (1548)     | 3.60 ± 0.60     | 2.50              | –  |
| Typical Diet (1548a)  | 4.70 ± 0.10     | 4.16 ± 0.04       | 4.22 ± 0.04 <sup>21c</sup>                               |
| Oyster Tissue (1566b) | 4.00 ± 0.20     | 2.80 ± 1.20       | –  |
| Tomato (1573a)        | 33.9 ± 1.20     | 33.3 ± 0.70       | 32.4 ± 4.00 <sup>20b</sup>                               |
| Corn Bran (8433)      | 3.90 ± 0.40     | 2.80 ± 1.20       | 2.06 ± 0.06 <sup>22d</sup><br>4.50 ± 1.40 <sup>19e</sup> |

<sup>a</sup> PGAA method.

<sup>b</sup> PGAA  $k_0$ -method.

<sup>c</sup> PGAA  $k_0$ -method, average value of 4.15±0.02 (cold neutrons) and 4.28±0.07 (thermal neutrons).

<sup>d</sup> ICP-MS method.

<sup>e</sup> ICP-MS and ICP-AES, average value, where Corn Bran 8433 is RM.

## Conclusions

The biological samples used are NIST SRMs such as Peach Leaves (SRM 1547), Apple Leaves (SRM 1515), Tomato Leaves (SRM 1573a), Spinach Leaves (SRM 1570a), Total Diet (SRM 1548), Typical Diet (SRM 1548a), Oyster Tissue (SRM 1566b) and Corn Bran (SRM 8433). The measured values for high boron concentration such as SRM 1547, 1515, 1570a and 1573a are in good agreement with the certified values, but at a low concentration below 5 ppm such as SRM 1548, 1566b and 8433, present values were higher than the certified values.

\*

This research has been carried out under the Nuclear R&D program by the Ministry of Science and Technology, Republic of Korea.

## References

1. U. GUPTA, Boron and Its Role in Cop Production, CRC Press, FL, USA, 1993.
2. H. IKURA, K. TANOI, T. M. NAKANISHI, J. Radioanal. Nucl. Chem., 249 (2001) 499.
3. F. H. NIELSEN, Biol. Trace Elem. Res., 27 (1990) 599.
4. F. H. NIELSEN, Nutr. Today, 27 (1992) 6.
5. D. L. ANDERSON, W. C. CUNNINGHAM, T. R. LINDSTOM, J. Food Comp. Anal., 7 (1994) 59.
6. P. LANZA, G. MORTERA, Anal. Chim. (Rome) 73 (1983) 371.
7. A. E. PILLAY, M. PEISACH, J. Radioanal. Nucl. Chem., 151 (1991) 379.
8. C. P. RAAIJMAKERS, M. W. KONIJNENBERG, L. DEWIT, D. HARITZ, R. HUISKAMP, K. PHILIPP, A. SIEFERT, F. STECHER-RASMUSSEN, B. J. MÜNHEER, Acta Oncol., 34 (1995) 517.
9. D. W. NIGG, Intern. J. Radiat. Oncol. Biol. Phys., 28 (1994) 1121.
10. C. YONEZAWA, A. K. HAJIWOOD, Anal. Chem., 67 (1995) 446.
11. T. MATSUMOTO, O. AIZAWA, J. Radiat. Appl. Instr., A41 (1990) 897.
12. S. OHDE, A. A. RAMOS, H. OZAKI, H. SAWAHATA, T. OKAI, J. Radioanal. Nucl. Chem., 258 (2003) 431.
13. D. L. ANDERSON, W. C. CUNNINGHAM, T. R. LINDSTROM, R. TYLER, J. Food Comp. Anal., 7 (1994) 59.
- 14a. H. J. CHO, Y. S. CHUNG, Y. J. KIM, Nucl. Instr. Meth. B, will be published.
- 14b. Y. S. CHUNG, H. J. CHO, J. H. MOON, S. H. KIM, Y. J. KIM, Anal. Sci. Techn., 16 (2003) 391.
15. International Atomic Energy Agency, IAEA-TECDOC-619, 1991.
16. T. KOBAYASHI, K. KANDA, Nucl. Instr. Meth., 204 (1983) 525.
17. M. K. KUBO, Y. SAKAI, J. Nucl. Radiochem. Sci., Vol. 1 (2000) 83.
18. R. M. LINDSTROM, Fresenius J. Anal. Chem., 360 (1998) 322.
19. A. M. S. NYOMORA, R. N. SAH, P. H. BROWN, R. O. MILLER, Fresenius J. Anal. Chem., 357 (1997) 1185.
20. V. H. TAN, N. C. HAI, T. T. ANH, L. N. CHUNG, INDC(NDS)-411, 2000.
21. H. MATSUE, C. YONEZAWA, J. Radioanal. Nucl. Chem., 249 (2001) 11.
22. A. S. AL-AMMAR, E. REITZNEROVA, R. M. BARNES, J. Radioanal. Nucl. Chem., 244 (2000) 267.